SCANNING VOL. 34, 137–144 (2012)

A Statistical Model of Signal–Noise in Scanning Electron Microscopy

F. Timischl, M. Date, and S. Nemoto

JEOL Technics Ltd., Akishima-shi, Tokyo, Japan

Summary: A statistical model describing signal-noise generation and development along the signal formation process in a standard scanning electron microscope (SEM) using an Everhart–Thornley secondary electron detector is derived. Noise in the detector signal is modeled to originate from a cascade of five signal conversion stages. Based on the derived model, general conclusions are drawn concerning the total signal-to-noise ratio (SNR) at each stage, and the influence of each stage on the total SNR of the detector signal. The model is furthermore applied to a real-world SEM, and verified by experimental data. SCANNING 34: 137–144, 2012. © 2011 Wiley Periodicals, Inc.

Key words: noise, cascade, signal-to-noise ratio, scanning electron microscopy

Introduction

As for most imaging devices, noise has been a major issue in scanning electron microscopy (SEM) for many years. The difficulty in understanding noise in the SEM detector signal results from the fact that noise cannot be confined to a single noise source within the signal formation process. Noise arises at multiple stages in a SEM, each contributing its own noise component to the detector signal noise. Previous investigations have shown that these noise components have different statistical properties depending on the physical nature of their origin (Delaney and Walton, '66; Baumann and Reimer, '81; Fujioka *et al*., '85; Sim *et al*., 2003; Tileli *et al*., 2009).

In order to reduce noise (i.e. increase the signal-to-noise ratio (SNR)) in the SEM signal, one has to evaluate the degree of contribution of each noise component to the final detector signal.

It is well known that shot noise is the main factor limiting the SNR of the final SEM image (Smith and Oatley, '55; Everhart *et al*., '59; Sim *et al*., 2003). Everhart *et al*. ('59) discusses the influence of the energy dependency of the secondary electron emission coefficient on the SNR, and Baumann and Reimer ('81) compare the influence of different detector types on the total image noise.

While above works identify and analyze various sources of noise in the signal formation process of a SEM, none of them provides an exhaustive qualitative and quantitative analysis showing the development of noise within the signal path that allows estimation of the degree of influence of each signal formation stage on the total SNR of the SEM detector signal.

The purpose of this work is to provide a systematical, theoretical and experimental approach to answer this question. A statistical model of the signal- and noise-generation process in a high-vacuum SEM is derived. The model shows how the SNR develops from one signal conversion stage to another, giving a qualitative and quantitative estimate of the influence of each stage on the total SNR of a SEM detector signal. The proposed noise model is verified using experimental data.

Materials and Methods

After a generalized theoretical analysis, investigations are performed with respect to a JEOL JSM-6610LV SEM (Tokyo), which is also used for the experimental verification. The JSM-6610LV employs a tungsten emitter and an Everhart–Thornley (ET)-detector for secondary electron imaging in the high-vacuum mode.

The 5-Stage Noise Model

The signal generation and conversion process in a SEM can be modeled to consist of five cascaded signal conversion stages as shown in Figure 1, where

Address for reprints: F. Timischl, JEOL Technics Ltd., 2-6-38 Musashino, Akishima-shi, Tokyo 196-0021, Japan
E-mail: ftimisch@jeol.co.jp

Received 29 May 2011; Accepted with revision 23 July 2011

DOI 10.1002/sca.20282
Published online 6 September 2011 in Wiley Online Library (wileyonlinelibrary.com)

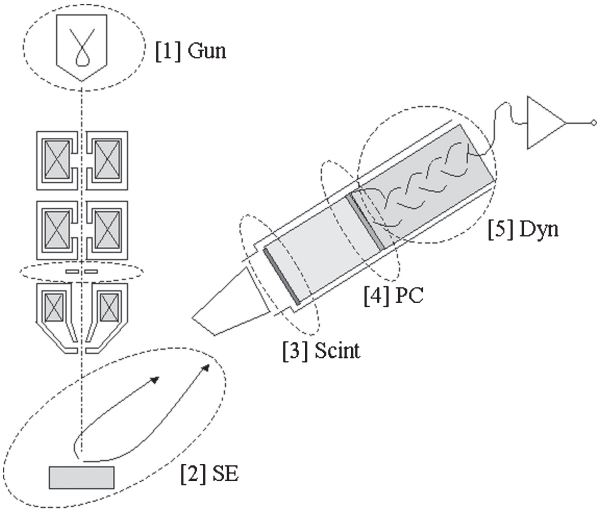

Fig 1. Basic noise model consisting of five signal conversion stages excluding amplifier noise.

the numbers in square brackets denote the position of each stage within the entire signal conversion process: [1] *Gun* denotes the generation of the primary electron beam at the electron gun and its limitation by the objective lens aperture. [2] *SE* denotes the emission of secondary electrons at the specimen and their collection by the secondary electron detector's collector, assuming an ET-type detector. [3] *Scint* describes the scintillation process. Finally, the stages [4] *PC* and [5] *Dyn* describe the signal conversion by the photocathode of the photomultiplier tube (PMT) and the signal multiplication in the PMT.

Subdivision of the total signal transfer path leading to the 5-stage model as described above is made so that each stage represents a physical signal conversion process obeying specific statistical rules. While the objective lens aperture and the signal collection by the secondary electron detector's collector have significant influence on the signal amount, they do not change the signal's statistical behavior, which is determined by any preceding processes. For this reason, the aperture and the signal collection are each combined with their preceding stages [1] *Gun* and [2] *SE*, respectively.

The objective of the presented signal conversion model is to break down total detector noise in a SEM into its sources with emphasis on physical signal generation and conversion processes, namely the optical column and the detector. Electronic signal amplification and processing are omitted in order to comply with this objective.

Statistics of Cascaded Events

The noise model of Figure 1 corresponds to a sequence of cascaded events, each following its own statistical laws. Such a model can be generalized by a sequence of events, where μ_i and σ_i denote the expectation value and the standard deviation of the ith event. Under the assumption of constant μ_i and σ_i, the total expectation value and standard deviation at the kth event, $\mu_{\mathrm{tot}(k)}$ and $\sigma_{\mathrm{tot}(k)}$, can be expressed as follows (Shockley and Pierce, '38).

$$\mu_{\mathrm{tot}(k)} = \mu_1\mu_2\ldots\mu_{k-1}\mu_k \tag{1}$$

$$\sigma^2_{\mathrm{tot}(k)} = \mu_k^2\sigma^2_{\mathrm{tot}(k-1)} + \mu_{\mathrm{tot}(k-1)}\sigma_k^2 \tag{2}$$

It has to be noted that $\mu_{\mathrm{tot}(k-1)}$ and $\sigma_{\mathrm{tot}(k-1)}$ in Equation (2) are the total expectation value and total standard deviation of the $(k-1)$th stage including all previous stages, while μ_k and σ_k denote the expectation value and the standard deviation of the kth stage alone.

The approach presented by Burle Technologies ('80) leads from the recursive form of Equation (2) to the following expression.

$$\sigma^2_{\mathrm{tot}(k)} = (\mu_1\mu_2\ldots\mu_k)^2 \cdot \left(\frac{\sigma_1^2}{\mu_1^2} + \frac{\sigma_2^2}{\mu_1\mu_2^2} + \frac{\sigma_3^2}{\mu_1\mu_2\mu_3^2} + \ldots + \frac{\sigma_k^2}{(\mu_1\mu_2\ldots\mu_{k-1})\mu_k^2}\right) \tag{3}$$

We will use the definition of SNR in Equation (4) in the following analysis and its experimental verification.

$$\mathrm{SNR} = \frac{\mu_i}{\sigma_i} \tag{4}$$

Substituting Equations (1) and (3) into Equation (4), one can calculate the total SNR, $\mathrm{SNR}_{\mathrm{tot}(k)}$ for any cascaded statistical process consisting of k single stages.

$$\mathrm{SNR}_{\mathrm{tot}(k)} = \left(\frac{\sigma_1^2}{\mu_1^2} + \frac{\sigma_2^2}{\mu_1\mu_2^2} + \frac{\sigma_3^2}{\mu_1\mu_2\mu_3^2} + \ldots + \frac{\sigma_k^2}{(\mu_1\mu_2\ldots\mu_{k-1})\mu_k^2}\right)^{-\frac{1}{2}} \tag{5}$$

Statistical Representation of the Basic Noise Model

The 5-stage model of Figure 1 can be represented in the form of Figure 2 to emphasize its cascaded nature, where each stage denotes a statistically governed signal conversion process.

The expectation value of the first stage, [1] *Gun* is given by

$$\mu_{\mathrm{Gun}} = \mu_{\mathrm{Gun\_0}} \cdot c_{\mathrm{Ap}} \tag{6}$$

where $\mu_{\mathrm{Gun\_0}}$ is the expectation value of the electron gun, and c_{Ap} is a constant factor describing the primary current limitation by the object lens aperture, which does not have to be treated as an

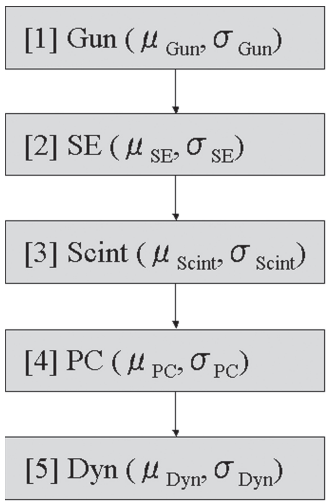

Fig 2. The 5-stage noise model of Figure 1 in a generalized cascade representation.

independent stage as explained above. σ_{Gun} is the standard deviation of the first stage, describing the statistical fluctuations of the primary electron beam below the objective lens aperture.

Analogously, the expectation value of the second stage, [2] SE can be expressed by

$$\mu_{\mathrm{SE}} = \mu_{\mathrm{SE\_0}} \cdot c_{\mathrm{Col}} \tag{7}$$

where $\mu_{\mathrm{SE\_0}}$ is the expectation value of the secondary electron emission process (the secondary electron yield), and c_{Col} is a constant factor representing the collection efficiency of the detector's electron collector. The standard deviation of the second stage is given by σ_{SE}. In this work, we assume a constant $\mu_{\mathrm{SE\_0}}$ for simplicity. The influence of the energy dependency of $\mu_{\mathrm{SE\_0}}$ on the total SNR is described in Everhart *et al.* ('59).

The expectation values and standard deviations of the stages [3] *Scint*, [4] *PC*, and [5] *PMT* are denoted by μ_{Scint} and σ_{Scint}, μ_{PC} and σ_{PC}, and μ_{Dyn} and σ_{Dyn}, respectively.

Substitution of the above defined parameters into Equation (5) gives the following equation for the 5-stage cascaded noise model of Figures 1 and 2.

$$\mathrm{SNR}_{\mathrm{tot}(5)} = \left(\frac{\sigma_{\mathrm{Gun}}^2}{\mu_{\mathrm{Gun}}^2} + \frac{\sigma_{\mathrm{SE}}^2}{\mu_{\mathrm{Gun}}\mu_{\mathrm{SE}}^2} + \frac{\sigma_{\mathrm{Scint}}^2}{\mu_{\mathrm{Gun}}\mu_{\mathrm{SE}}\mu_{\mathrm{Scint}}^2} + \frac{\sigma_{\mathrm{PC}}^2}{\mu_{\mathrm{Gun}}\mu_{\mathrm{SE}}\mu_{\mathrm{Scint}}\mu_{\mathrm{PC}}^2} + \frac{\sigma_{\mathrm{Dyn}}^2}{\mu_{\mathrm{Gun}}\mu_{\mathrm{SE}}\mu_{\mathrm{Scint}}\mu_{\mathrm{PC}}\mu_{\mathrm{Dyn}}^2} \right)^{-\frac{1}{2}} \tag{8}$$

Equation (8) is an analytical expression of the total SNR of the 5-stage cascaded process, without any restrictions on the statistics involved. Equation (8) can easily be modified to express the total SNR at any other than the fifth stage by simply omitting the unneeded terms on the right side.

The Poisson Distribution Approximation

While electron emission at the electron gun is usually expressed using the Poisson distribution (Sim *et al.*, 2003), secondary electron emission at the specimen follows the so-called "compound Poisson distribution". However, since the effect of electric fields in the vicinity of the location of secondary electron emission can be neglected, the ordinary Poisson distribution can be used as a valid approximation (Shockley and Pierce, '38). Different from secondary electron emission, backscattered electron (BSE) emission is governed by the binomial distribution, which is caused by the fact that only one or zero BSE can be emitted for one incident electron (Baumann and Reimer, '81). Assuming that the major fraction of the signal collected by an outer-lens ET-type detector results from SE1 (secondary electrons generated directly by the electron beam), we limit our analysis to the Poisson distributed case.

Both the scintillation process and the photon-electron conversion in the photomultiplier's photocathode can be treated as Poisson processes (Burle Technologies, '80; Gilmore, '92). Electron multiplication by the dynodes of the photomultiplier is again a compound Poisson process, which can be well approximated by the ordinary Poisson distribution as long as the voltage applied to the PMT is relatively low (Shockley and Pierce, '38).

We can therefore assume that each signal conversion process in our 5-stage noise model of Figure 2 can be treated as a Poisson process. This assumption simplifies the preceding analysis considerably.

The standard deviation σ of a Poisson distributed process with expectation value μ is given by

$$\sigma = \sqrt{\mu} \tag{9}$$

With the assumption of a Poisson process in every stage and Equation (9), Equation (5) can be simplified as follows.

$$\mathrm{SNR}_{\mathrm{tot}(k)} = \left(\frac{1}{\mu_1} + \frac{1}{\mu_1\mu_2} + \frac{1}{\mu_1\mu_2\mu_3} + \cdots + \frac{1}{(\mu_1\mu_2 \ldots \mu_{k-1})\mu_k} \right)^{-\frac{1}{2}} \tag{10}$$

Substitution of the expectation values and standard deviations with the proposed notations for our 5-stage model into Equation (10) gives for the total SNR at the fifth stage under the assumption of a Poisson process in every stage

$$\mathrm{SNR}_{\mathrm{tot}(5)} = \left(\frac{1}{\mu_{\mathrm{Gun}}} + \frac{1}{\mu_{\mathrm{Gun}}\mu_{\mathrm{SE}}} + \frac{1}{\mu_{\mathrm{Gun}}\mu_{\mathrm{SE}}\mu_{\mathrm{Scint}}} + \frac{1}{\mu_{\mathrm{Gun}}\mu_{\mathrm{SE}}\mu_{\mathrm{Scint}}\mu_{\mathrm{PC}}} + \frac{1}{\mu_{\mathrm{Gun}}\mu_{\mathrm{SE}}\mu_{\mathrm{Scint}}\mu_{\mathrm{PC}}\mu_{\mathrm{Dyn}}} \right)^{-\frac{1}{2}} \tag{11}$$

Equation (11) consists of five terms, one for each stage in our cascaded noise model. The number of parameters constituting each term increases with the order of the corresponding stage. This directly reflects the fact that stages with lower order (at "earlier" stages within the cascade) have higher influence on the total SNR than stages with higher order. This is in accordance with well-known empirical results as described in Smith and Oatley ('55) and Sim *et al*. (2003).

Figure 3 shows the dependence of the total SNR at the kth stage, $\mathrm{SNR}_{\mathrm{tot}(k)}$ with stage order, i.e. the development of $\mathrm{SNR}_{\mathrm{tot}(k)}$ within the total signal conversion cascade. $\mathrm{SNR}_{\mathrm{tot}(k)}$ values are calculated using Equation (10), where the same expectation value μ is assumed for all stages.

Other questions of major interest are how much each stage in the cascade contributes to the total noise at the final stage (expressed by $\mathrm{SNR}_{\mathrm{tot}(5)}$), and how $\mathrm{SNR}_{\mathrm{tot}(5)}$ can be increased efficiently.

The data points of Figure 4 show the increase in $\mathrm{SNR}_{\mathrm{tot}(5)}$, if μ of only the stage with index k is doubled. The following important conclusions can be drawn from Figures 3 and 4.

(1) $\mathrm{SNR}_{\mathrm{tot}(k)}$ decreases with stage order k for all possible values of μ.

(2) Both the absolute value of $\mathrm{SNR}_{\mathrm{tot}(k)}$ as well as the rate of $\mathrm{SNR}_{\mathrm{tot}(k)}$ decrease with stage order depend on the expectation value μ of each stage. Generally, higher expectation values μ lead to higher $\mathrm{SNR}_{\mathrm{tot}(k)}$ with less change of its absolute value with stage order k.

(3) Increase of the expectation value μ of any stage within the signal conversion cascade leads to increase in $\mathrm{SNR}_{\mathrm{tot}(5)}$.

(4) Stages with lower order (lower k) have higher influence on $\mathrm{SNR}_{\mathrm{tot}(5)}$.

(5) Except the first stage, the amount of $\mathrm{SNR}_{\mathrm{tot}(5)}$-increase depends on the absolute value of the increased μ and not only on its ratio of increase.

(6) The higher an expectation value is, the lower is the effect on $\mathrm{SNR}_{\mathrm{tot}(5)}$, if it is changed.

Above equations can be summarized in the following form for generalization purposes. The total SNR at the kth stage, $\mathrm{SNR}_{\mathrm{tot}(k)}$ of a cascade of arbitrary stage number m, where each stage exhibits Poisson statistics is given as

$$\mathrm{SNR}_{\mathrm{tot}(k)} = \left(\frac{\prod_{i=1}^{k} \mu_i}{1 + \sum_{i=2}^{k} \prod_{j=i}^{k} \mu_j} \right)^{\frac{1}{2}} \tag{12}$$

with $1 \le k \le m$

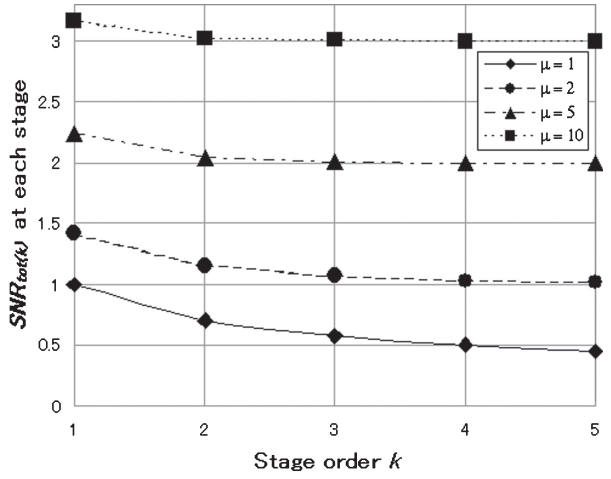

Fig 3. $\mathrm{SNR}_{\mathrm{tot}(k)}$ calculated from Equation (10) in dependence of the stage order k under the assumption of equal expectation values μ for each stage.

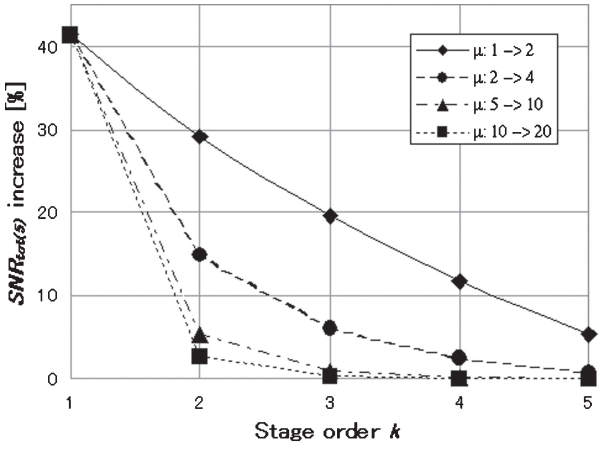

Fig 4. The increase of $\mathrm{SNR}_{\mathrm{tot}(5)}$ under the assumption of equal expectation values μ for each stage, if μ is increased by 100% at each stage separately.

In contrast, increase in the expectation value at only the kth stage by a factor a gives

$$\mathrm{SNR}_{\mathrm{tot}(m)\_a_k} = \left(\frac{a \prod_{i=1}^{m} \mu_i}{1 + a \sum_{i=2}^{k} \prod_{j=i}^{m} \mu_j + \sum_{i=k+1}^{m} \prod_{j=i}^{m} \mu_j} \right)^{\frac{1}{2}} \quad \text{with } 1 \le k \le m \tag{13}$$

Thus, Figure 4 shows the case $k = 1,2,3,4,5$ and $m = 5$.

Application to the JEOL JSM-6610LV and Experimental Verification

First, expectation values for each signal transfer stage obtained from experiments and simulations (with respect to the JSM-6610LV) are substituted into Equation (11) to obtain figures analogous to Figures 3 and 4 for the JSM-6610LV.

Observation conditions for the experiments are chosen as shown in Table I. All expectation values are calculated with respect to Table I, i.e. they correspond to the experimental conditions to allow comparison of the theory with the experiment.

SNR in the Signal Conversion Cascade of a Realistic SEM

The expectation value of the first stage, μ_{Gun}, can be obtained approximately by measuring the beam current right below the objective lens aperture. We adjusted the emission current in order to obtain a value of 25 pA as required to match the conditions of Table I. Since $1A = 6.242 \times 10^{18}$ electrons per second, and the time interval t corresponding to one pixel in the scan mode under consideration is $t = 3.2 \times 10^{-7}$ s, this gives $\mu_{\mathrm{Gun}} = 49.9$ El/t as the expectation value for the first stage.

The specimen used for the experiments is a polished copper plate. This gives an electron yield, $\mu_{\mathrm{SE\_0}} = 0.38$ (Seiler, '83). $\mu_{\mathrm{SE\_0}}$ is a dimensionless quantity. The collection efficiency of the secondary electron detector's collector was obtained by extensive simulations (which are not the object of this paper) using the software package Elec3D by E. Munro ('89), leading to a value $c_{\mathrm{Col}} = 0.2$ for the observation conditions in Table I. This value is in close accordance with those presented in Muellerova and Konvalina (2009). This results in the expectation value of the second stage $\mu_{\mathrm{SE}} = 0.076$.

TABLE I Observation conditions for the experiments

Issue	Value	Unit
Beam current below the objective lens aperture	25	pA
Acceleration voltage	20	kV
Objective lens aperture diameter	30	μm
Working distance	10	mm
Magnification	100	–
Specimen secondary electron yield (Copper)	0.38	–
Collector voltage	40	V
Scan frame rate	6.67	s^{-1}

The expectation value of the third stage is the quantum efficiency of the scintillator. For a P47-scintillator (9.2 generated photons per 1 keV impinging electron), which was used for the experiment, where a bias voltage of 9 kV was applied to the scintillator's surface with respect to the specimen, this gives $\mu_{\mathrm{Scint}} = 82.8$. It is assumed for simplicity that all detected secondary electrons have the same energy at the incident of detection. As will be explained in the following, the expectation value of the third stage was decreased by 50% for the reference signal in the experiment. In order to comply with the experiment, a value $\mu_{\mathrm{Scint}} = 41.4$ was therefore used in the following calculation.

The quantum efficiency of the photocathode is given by 110 μA/lm according to the manufacturer's data. Considering the definition of the lumen, this gives $\mu_{\mathrm{PC}} = 0.17$ as the expectation value of the fourth stage.

The fifth stage is the multiplication factor of the dynode cascade in the photomultiplier. This value can again be obtained from the manufacturer's data (the anode sensitivity divided by the cathode sensitivity), which gives $\mu_{\mathrm{Dyn}} = 2.6 \times 10^6$.

Substitution of the expectation values of above into Equation (10) gives $\mathrm{SNR}_{\mathrm{tot}(k)}$ at the kth stage for the JSM-6610LV (Fig. 5). Considering the difficulty in measuring $\mathrm{SNR}_{\mathrm{tot}(k)}$ at any stage except

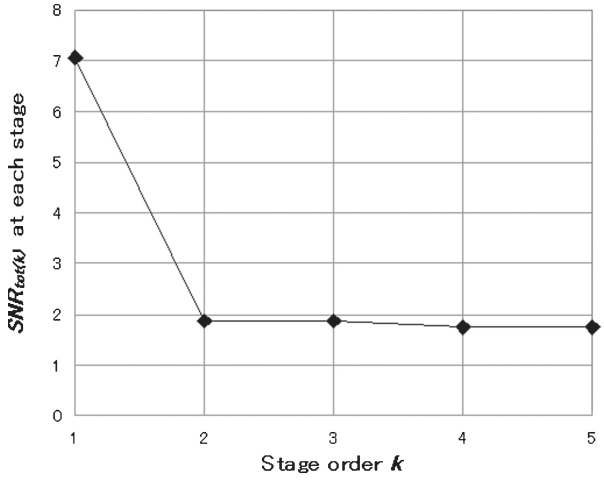

Fig 5. $\mathrm{SNR}_{\mathrm{tot}(k)}$ in dependence of the stage order k calculated from Equation (10) using realistic expectation values for the JSM-6610LV.

the last one, the experimental verification is only given for the last stage as follows.

Contribution of Each Stage on the Total SNR

Investigation of the influence of each stage on $SNR_{tot(5)}$ for the JSM-6610LV is performed analogously to the general analysis of above. After obtaining a reference $SNR_{tot(5)}$ by using the expectation values of above, we separately increase μ for the kth stage (for $k = 1,2,3,4,5$) by 100% and calculate the increase in $SNR_{tot(5)}$ for each case. The resulting graph is shown as the solid line in Figure 6.

The data in Figures 5 and 6 are in accordance with the general results of Figures 3 and 4. In particular, both figures show that $SNR_{tot(k)}$ decrease becomes negligible after the second stage ($k = 2$), and that the first and the second stage have by far the highest influence on the absolute value of $SNR_{tot(5)}$. Both phenomena are caused by the relatively low value of μ_{SE} and the relatively high value of μ_{Scint}.

It is important to notice that these results are still theory-based, since $SNR_{tot(k)}$ and $SNR_{tot(5)}$ are calculated using the theory derived above.

Signal and noise measurement was carried out employing two different experimental setups for comparison purposes.

The first employs the approach described by Tileli *et al*. (2009). The output of the photomultiplier tube was connected to a preamplifier, which is the standard configuration of the JSM-6610LV. The preamplifier output was connected in parallel to the microscope's image acquisition system, a digital voltmeter (Keithley, 2000, signal data acquisition), and a spectrum analyzer (Advantest R3131A, noise data acquisition). For noise measurement, the spectrum analyzer's noise measurement and marker functions were used. The noise level was measured at 60 kHz at a RBW of 300 Hz. Under the condition of white noise, the obtained value is proportional to the total noise level integrated across all frequencies. Signal values were obtained in mV, noise in $\mu V/(Hz^{1/2})$.

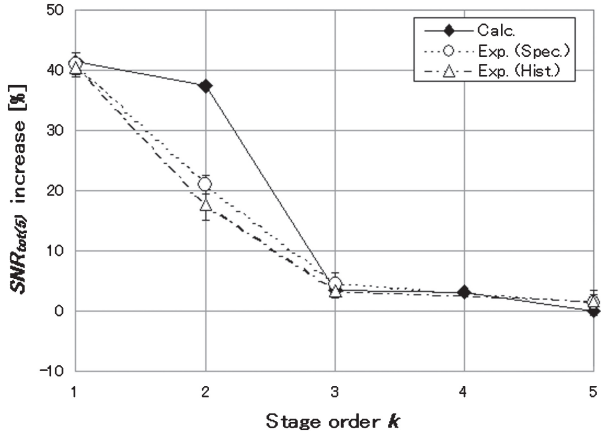

Fig 6. The increase of $SNR_{tot(5)}$ if each stage's μ is separately increased by 100%. Comparison of theoretically and experimentally obtained $SNR_{tot(5)}$ values.

The second experimental setup uses histogram plots of images acquired with the JSM-6610LV under the described conditions. Since a featureless polished copper plate was used as a specimen, the histogram consists of a single peak. While the expectation value μ is simply given by the horizontal position of this peak, the standard deviation σ can be easily obtained via the full width at half maximum (FWHM) using

$$\mathrm{FWHM} = 2\sqrt{2 \cdot \ln(2)} \cdot \sigma \approx 2.35 \cdot \sigma \qquad (14)$$

Although Equation (14) is strictly valid only for Gaussian-distributed data, it can be used in the present case referring to the central limit theorem, which states that any distribution can be approximated by the Gaussian distribution under the condition of sufficiently large expectation values.

The following experimental procedure was performed for both experimental setups separately.

$SNR_{tot(5)}$ was calculated inserting the measured values into Equation (4). However, we confine experimental results to relative $SNR_{tot(5)}$ values, since the bandwidth of the measured data is unknown, which would be a requirement for obtaining absolute SNR values (Tileli *et al*., 2009).

In order to obtain experimental data for each stage's influence on $SNR_{tot(5)}$, we followed exactly the same approach that was taken to calculate the theoretical data of Figure 6.

In a first step, a neutral-density filter with 50% transmittance was placed between the secondary electron detector's light guide and the entrance window of the photomultiplier in order to reduce the amount of signal passed from the scintillator to the PMT by 50%. The reason for this modification (which is equivalent to the above μ_{Scint}-limitation by 50%) will become evident in the following. Using this detector setup and the observation conditions of Table I, signal and noise measurement was performed to obtain a reference-$SNR_{tot(5)}$ value.

In a second step, the expectation value (amount of signal) for each stage was doubled separately, and $SNR_{tot(5)}$ measured again as explained above. The increased values of $SNR_{tot(5)}$ at each stage compared to the reference value were used as the experimental values in Figure 6.

Doubling of the signal amount of the first stage, [1] *Gun* was done changing the condenser lens excitation to increase the beam current by 100%, which was measured with a faraday cup below the

object lens aperture and at the output of the PMT preamplifier for comparison.

Analogously, the 100% increase in expectation value of the second stage, [2] *SE* was realized by increasing the collection efficiency of the detector, since the specimen and the collection process together form the second stage. In concrete, the collector's bias voltage was increased from 40 to 244 V, giving exactly twice as much signal.

The statistics of the third stage, [3] *Scint* is governed by the scintillation process. Regarding the difficulties in realization of a scintillator with twice quantum efficiency (which was desired in this experiment) we decided to choose an upside-down approach, i.e. limiting the signal after the scintillator by 50% for the reference signal by inserting a neutral-density filter with 50% transmittance (as explained above), and removing it in the second step of the experiment in order to simulate doubled signal output of the scintillator.

As for the fourth stage, [4] *PC* we could not realize any experimental setup for doubling the expectation value of the photomultiplier's photocathode. The corresponding datapoints are therefore omitted in Figure 6.

The expectation value of the fifth stage, [5] *PMT* was increased by directly employing the photomultiplier's anode sensitivity. Compared to the PMT with anode sensitivity 284 A/lm, which was used for the reference signal, we used another PMT (of the same model) with anode sensitivity 619 A/lm, which corresponds to an increase in expectation value and signal by 118%. The deviation of expectation value increase from the desired 100% introduces a small error. However, regarding the low influence of the fifth stage on the change in $SNR_{tot(5)}$, we regard this error as negligible.

Results

Experimental data obtained by using the signal spectrum and the image histograms are denoted by *Exp.* (*Spec.*) and *Exp.* (*Hist.*) in Figure 6, respectively. *Exp.* (*Spec.*) gives a 41% increase in $SNR_{tot(5)}$, if the first stage's μ is increased by 100%. This $SNR_{tot(5)}$-increase drops to 21% for the second stage. After the second stage, the $SNR_{tot(5)}$-increase decreases to 4% for the third and 1% for the fifth stage, respectively. *Exp.* (*Hist.*) gives very similar data (40% for the first, 18% for the second, 3% for the third, and 1% for the fifth stage), indicating that the image histogram procedure is a sufficient experimental approach to the problem under consideration. We however regard the first experimental setup using the signal spectrum as the more reliable one for general noise measurement, since it eliminates any influence of the electronics and signal processing software.

Figure 6 shows good agreement between calculated and both sets of experimental data for the first, the third, and the fifth stage. The error bars in Figure 6 each correspond to one standard deviation under the condition of three repeated experiments for each stage.

The deviation of the theoretical value from the experimental ones at the second stage in Figure 6 has its origin in the approximate choice of μ_{SE} (refer to Fig. 4), which is confined to SE1 in the present analysis. Neglecting SE3 contributes to this deviation as follows.[1] SE3 are generated by a two-stage BSE-SE3 cascade within the second stage in parallel with the SE1 generation process, where BSE are assumed to be binomially distributed and the SE3 emission itself follows a Poisson distribution (with a BSE yield of 0.34 (copper specimen) and an SE3 yield of 0.38 (iron specimen chamber and objective lens) according to Seiler, '83). The obtained expectation value and standard deviation of the SE3 are combined with those of the SE1 following standard rules for additive statistical events. Substituting these values into Equation (8) lowers the theoretical value of $SNR_{tot(5)}$-increase at the second stage in Figure 6 by merely 2%, leaving all other stages unchanged.[2] SE3 are therefore negligible under the assumption of constant electron energies, which this work is confined to.

One possible reason for the deviation at the second stage in Figure 6 is the BSE energy distribution, which leads to a considerable variation of the SE3 yield and standard deviation, and therefore of μ_{SE} and σ_{SE}. Additionally, electron collection efficiency is not necessarily the same for SE1 and SE3 (as assumed in the present analysis). Finally, the SE1 yield is strongly dependent on oxide and contamination layers on the specimen's surface (Seiler, '83). A more sophisticated model for the second stage including the above effects is object to further studies.

Finally, it has to be noted that this work exclusively deals with the high-vacuum SEM. A detailed treatment of noise in environmental scanning electron microscopy requires consideration of other parameters such as initial beam energy,

[1] BSE are not included in this estimation since they account for only a few percent of the total secondary electron detector signal, as compared to several ten percent for the SE3 (Everhart, '59).

[2] Equation (8) is used with regard to the BSE-SE3 cascade, which deviates from the Poisson distribution. However, substituting the expectation value of the combined signal of SE1 and SE3 as obtained above into Equation (11) changes the value of $SNR_{tot(5)}$-increase of the second stage by only 1% (as compared to the calculation using Equation (8)), which indicates that the Poisson approximation still holds.

specimen-detector distance, and gas pressure. This topic is covered in detail by Tileli *et al*. (2009).

Conclusion

Based on the statistical theory for cascaded events, an analytical noise model for the signal generation process in a conventional SEM has been established. The model divides the signal path into the following five steps: [1] *Gun*, [2] *SE*, [3] *Scint*, [4] *PC*, and [5] *Dyn*. Signal conversion at each stage is assumed to be Poisson distributed. The derived model clearly shows the development of the total SNR (expressed by $SNR_{tot(k)}$) from one stage to another in dependence on expectation values, and therefore explains the contribution of each stage to the total SNR of the final detector signal (expressed by $SNR_{tot(5)}$). The major general conclusions are: (i) $SNR_{tot(k)}$ of the kth stage decreases with stage order k, and (ii) the influence of each stage on $SNR_{tot(5)}$ decreases with stage order. Application of the theoretical model to the JEOL JSM-6610LV shows that the first two stages have by far the highest influence on $SNR_{tot(5)}$, i.e. they carry the highest potential for $SNR_{tot(5)}$-increase. The proposed theory was verified by experimental data.

References

Baumann W, Reimer L. 1981. Comparison of the noise of different electron detection systems using a scintillator-photomultiplier combination. Scanning 4:141–151.

Burle Technologies. 1980. Photomultiplier Handbook. Lancaster: Burle Technologies.

Delaney CFG, Walton PW. 1966. Measurement of the statistics of secondary electron emission. IEEE Trans Nucl Sci 13:742–746.

Everhart TE, Wells OC, Oatley CW. 1959. Factors affecting contrast and resolution in the scanning electron microscope. J Electron Control 7:97–111.

Fujioka H, Nakamae K, Ura K. 1985. Signal-to-noise ratio in the stroboscopic scanning electron microscope. J Phys E Sci Instrum 18:598–603.

Gilmore R. 1992. Single Particle Detection and Measurement. London/Washington, DC: Taylor & Francis Ltd.

Muellerova I, Konvalina I. 2009. Collection of secondary electrons in scanning electron microscopes. J Microscopy 236:203–210.

Seiler H. 1983. Secondary electron emission in the scanning electron microscope. J Appl Phys 54:R1–R18.

Shockley W, Pierce JR. 1938. A theory of noise for electron multipliers. Proc Inst Radio Eng 26:321–332.

Sim KS, Thong JTL, Phang JCH. 2003. Effect of shot noise and secondary emission noise in scanning electron microscope images. Scanning 26:36–40.

Smith KCA, Oatley CW. 1955. The scanning electron microscope and its field of application. British J Appl Phys 6:391–399.

Tileli V, Knowles WR, Toth M, Thiel BL. 2009. Noise characteristics of the gas ionization cascade used in low vacuum scanning electron microscopy. J Appl Phys 106:014904-014901-014904-8.